

Supplemental Tables and Figures

Table S1. Related to Figure 3. Root-from-stump in different *glr* single mutants

Genotype	root regenerated	not regenerated	total root tested	Regeneration rate (%)
Col-0	31	19	50	62.0
<i>glr 1.2</i>	33	17	50	66.0
<i>glr 1.4</i>	35	15	50	70.0
<i>glr 3.3</i>	26	24	50	52.0

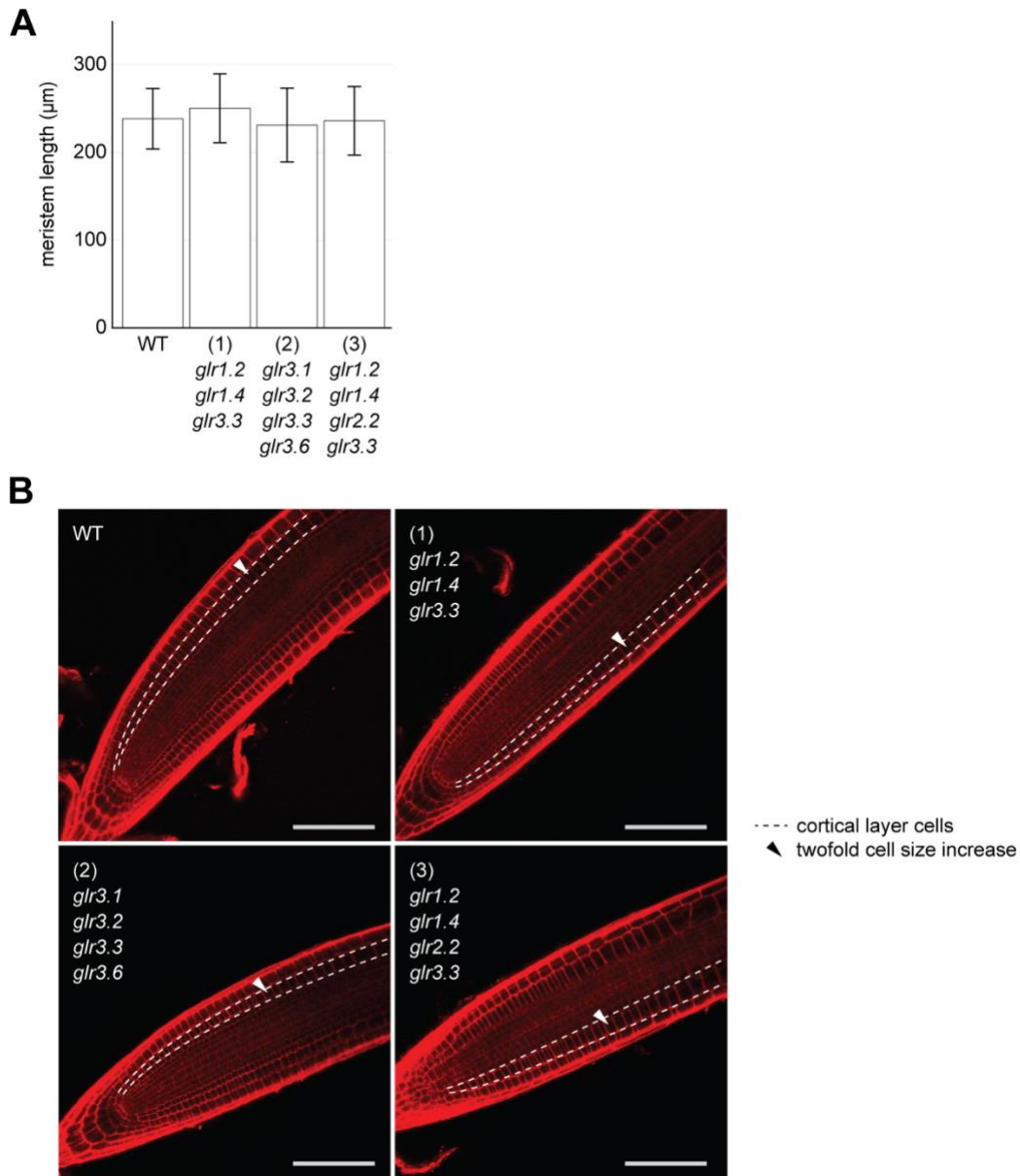


Figure S1. Related to Figure 3. GLR mutants have a normal meristem size. **A.** Quantitative analysis of meristem size in wild type and mutants, with no change in meristem size detected ($n > 20$, $p > 0.24$). The upper boundary of the meristem was defined as the position of the cell that showed a two-fold or more cell size increase compared to its distal neighbor in the cortical layer. **B.** Representative images of the different genotypes with cortex cell file enclosed by dashed lines and arrow head pointing the beginning of the transition zone. Scale bars=100µm.

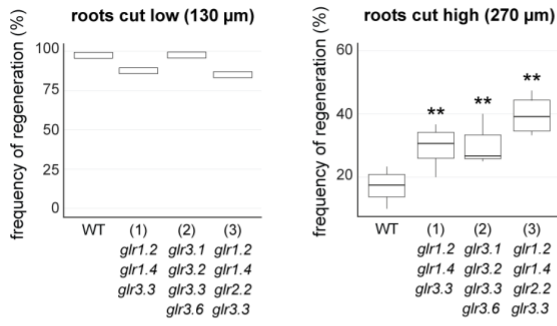
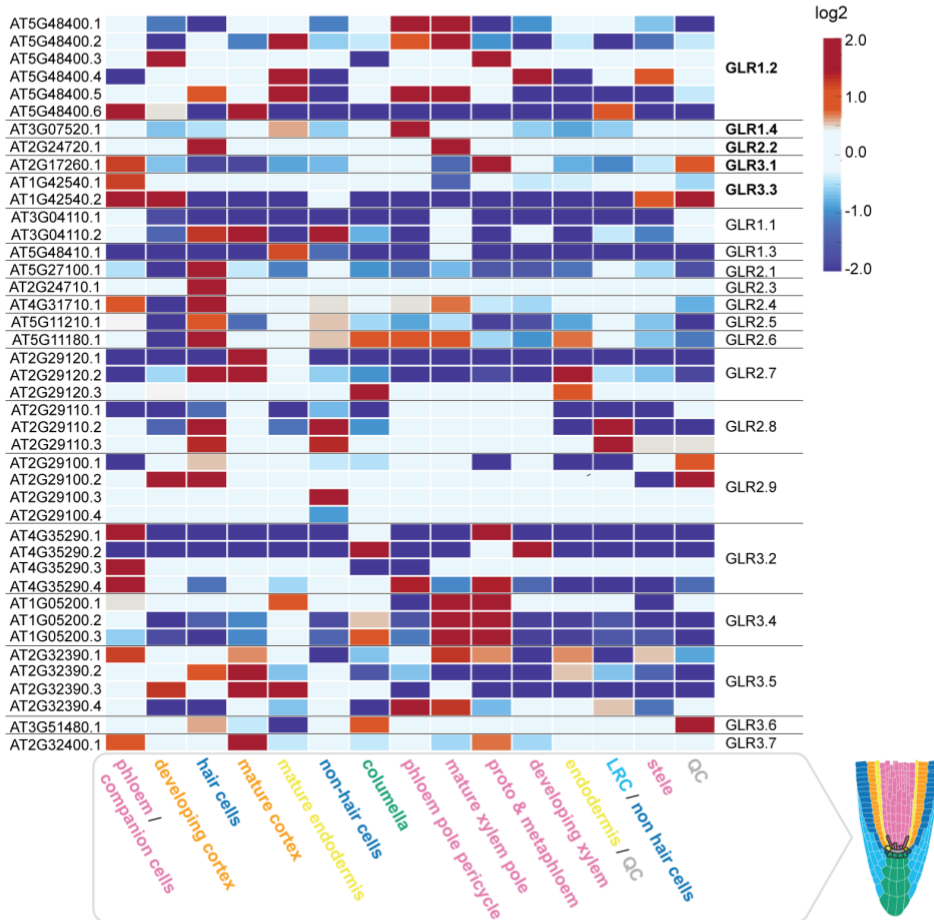
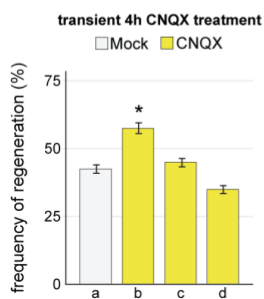
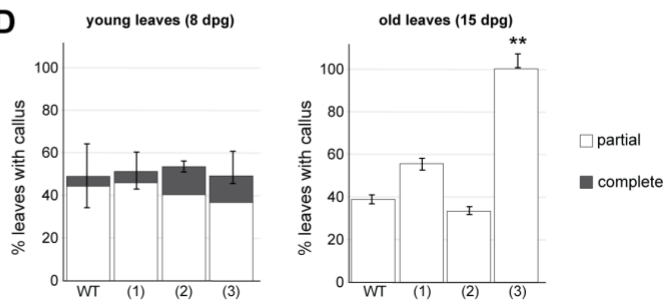
A**B****C****D**

Figure S2. Related to Figure 3. Regeneration responses in different conditions and assays. **A.** Root regeneration frequency in the *glr* mutants is greatly affected by the position of the cut. (1) *glr1.2/1.4/3.3*, (2) *glr3.1/3.2/3.3/3.6* and (3) *glr1.2/1.4/2.2/3.3*. At low cuts, in the early meristem, no difference among samples was observed (left graph, n=40). However, at high cuts, where cells are older, the *glr1.2/1.4/3.3* and *glr1.2/1.4/2.2/3.3* mutants regenerate better than wild type (on right, note the graph presented from Figure 3A shown again here for comparison). **B.** *GLR* paralogs show complementary expression patterns in the Arabidopsis root. Different rows of the same gene represent alternative splice isoforms. **C.** Root-from-stump under CNQX transient treatment (4 h exposure) or transient withdrawal (transfer to standard plates after 4 h exposure). None of the transient treatments increased regeneration efficiency over Mock treatment. a=cut and transfer to Mock; b=cut and transfer to CNQX; c=4h on Mock and transfer to CNQX; d=4h on CNQX and transfer to Mock. The error bars are proportional to the standard error of the pooled percentage computed using binomial distribution (Chi-square test; n=40, *p<0.03). **D.** Comparison of callus formation on young (10 dpv) and old (15 dpv) leaves from the *GLR* mutants (on right, graph presented in Figure 3G shown for comparison). Differences in the phenotype of *GLR* mutants are only observed in older tissues. When young leaves were used, no significant difference in callus formation efficiency was observed among genotypes (n>76 for each genotype). Callus formation on part of the leaf (Partial) or on the whole leaf (Complete) is indicated. In older leaves, complete callus formation was not observed.

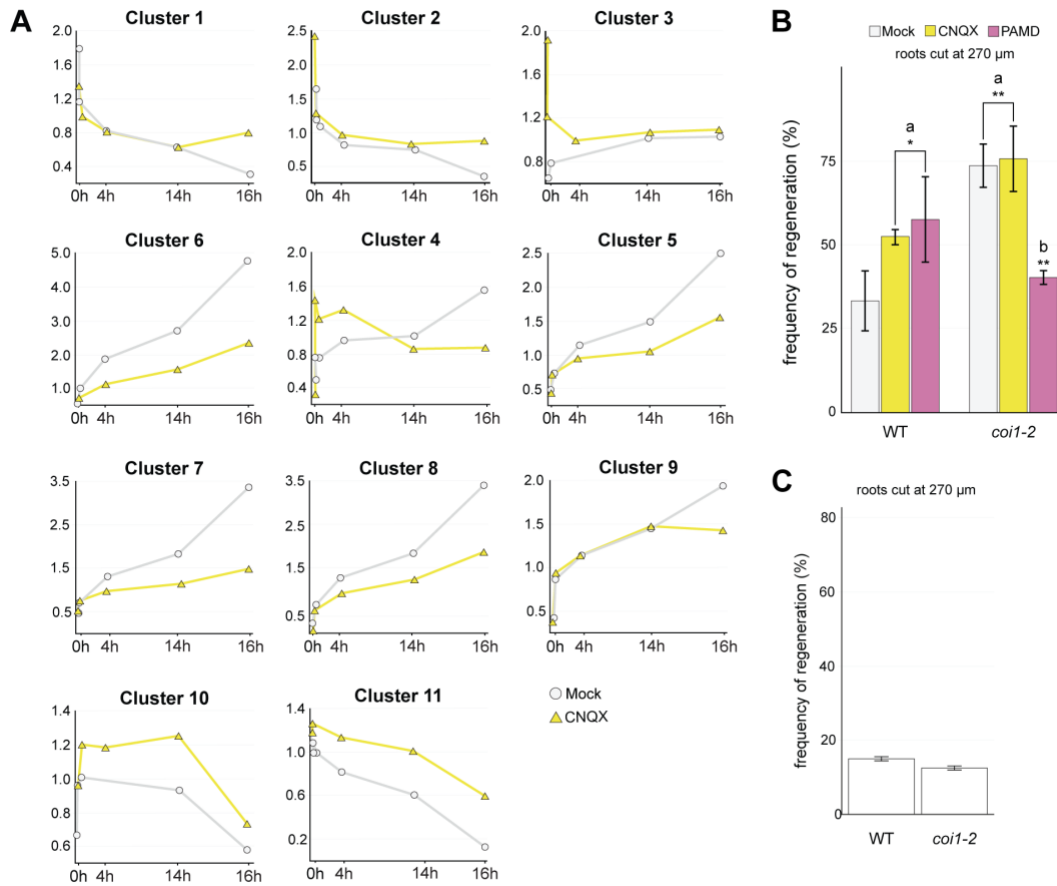


Figure S3. Related to Figure 4. Effects of CNQX on gene expression. **A.** The 11 gene expression profiles obtained from ImpulseDE analysis of the RNA-seq data, showing differences between CNQX- and Mock-treated samples. Time post cut is represented on the x-axis. For Gene Ontology enrichment analysis of the 11 clusters see Supplemental Table 2. **B.** Root-from-stump regeneration effects of the *coi1* mutant, showing increased regeneration in this trial and insensitivity to PAMD in the *coi1* mutant (Chi-square test; $n > 40$; ^a significant difference with respect to Col-0 Mock, $*p < 10^{-6}$, $**p < 10^{-10}$; ^b significant difference with respect to *coi1-2* Mock, $**p < 10^{-12}$). **C.** Replicate of *coi1-2* root-from-stump assay where regeneration frequency compared to wild type levels shows no significant difference between wild type and *coi1-2* contrary to B (Chi-square test; $n = 40$, not significant).

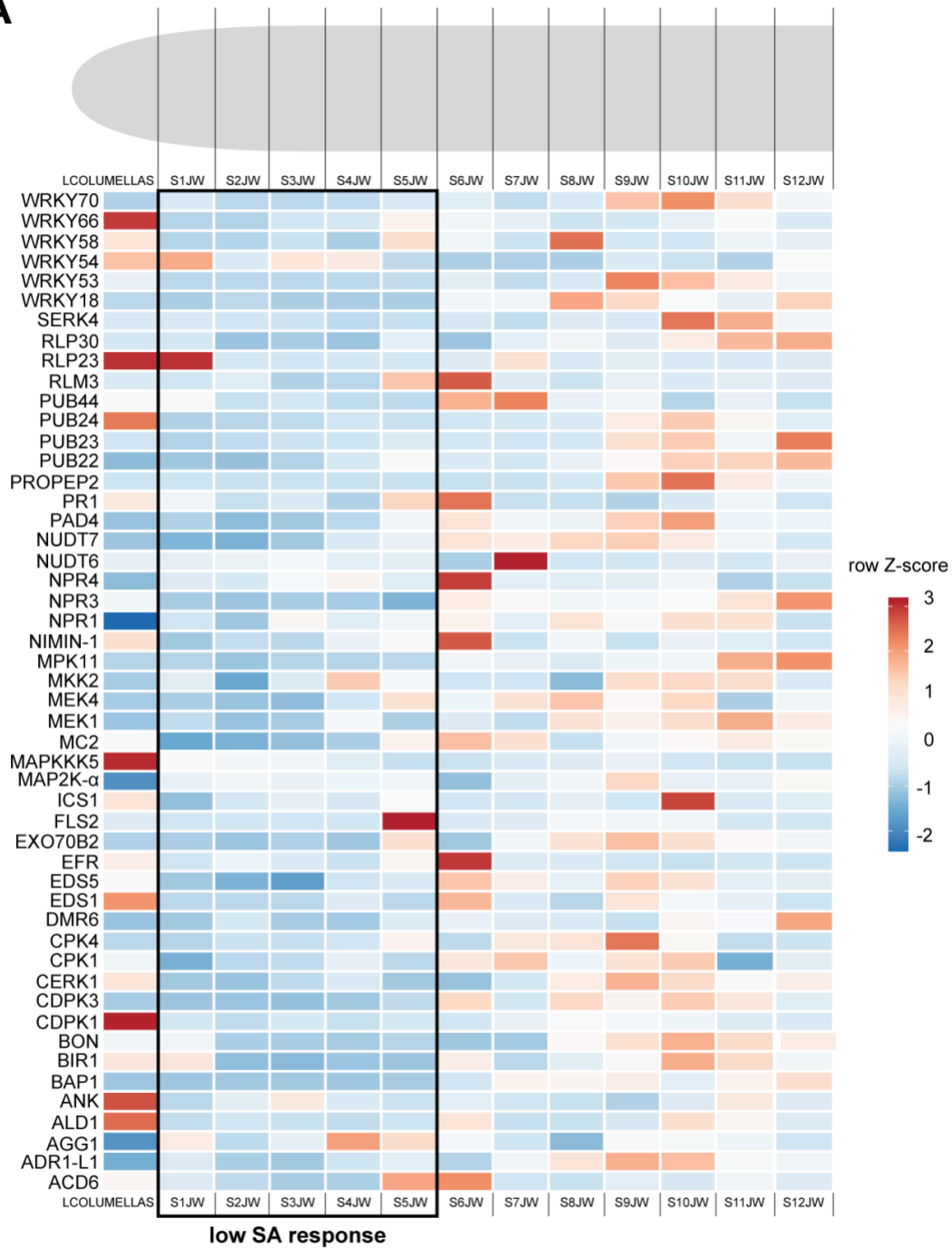
A

Figure S4. Related to Figure 4. Expression of SA responsive markers along the root meristem maturation axis. Relative expression of SA response markers in successive longitudinal sections of the root, showing low SA responses in the basal meristem. Leftmost column is the columella at the root tip,

with successive slices taken toward the more proximal (mature) sections of the root. Row normalized by z score. Data is from Brady et al. 2007.

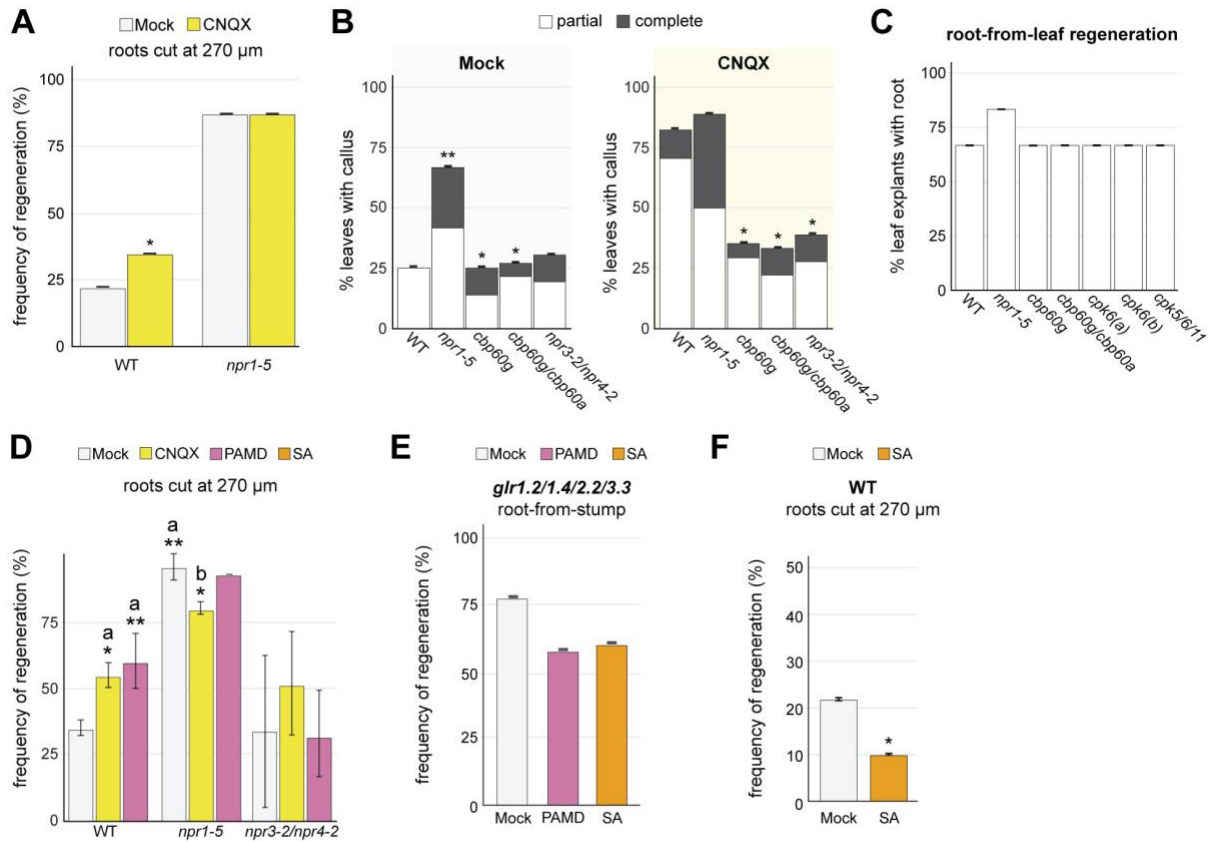
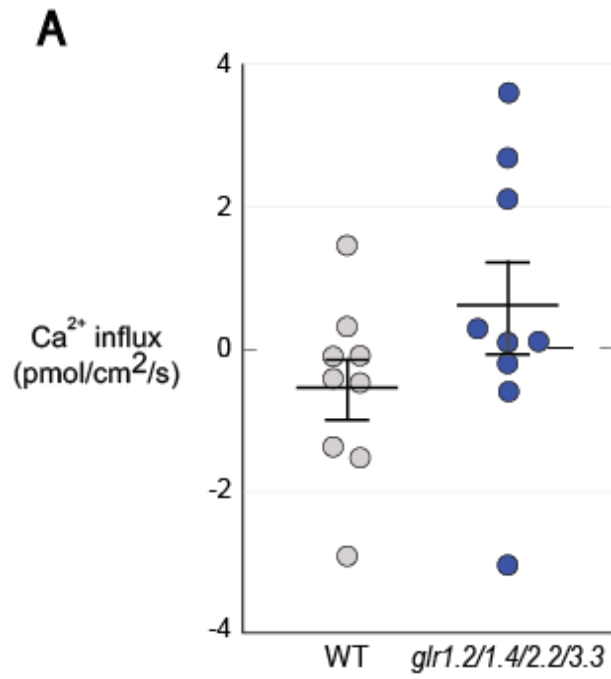


Figure S5. Related to Figure 5. Mutants from the SA pathway tested for regeneration in different assays. **A.** The *npr1-5* mutant is insensitive to CNQX constitutive post-injury treatment in compared to wild type with regards to regeneration (Chi-square test; $n \geq 40$; $*p < 0.03$). **B.** Callus regeneration assay using five different mutants involved in SA response. *npr1-5* showed higher callus formation rates compared to Col-0 (left), but insensitivity to constitutive post-injury CNQX treatment (right). Other SA pathway mutants show subtle improvement in complete callus formation. The error bars are proportional to the standard error of the pooled percentage computed using binomial distribution. Tests represent number of plants with callus present, either complete or partial. (Chi-square test; $n \geq 12$; $*p < 0.01$; $**p < 0.10^{-9}$). **C.** In the root-from-leaf experiment, only *npr1-5* showed a tendency toward higher regeneration frequency compared to wild type ($n=12$) but did not show a significant difference. Error bars are proportional to the standard error of the pooled percentage. **D.** Regeneration frequency of wild type and *npr* mutants under different chemical treatments, where *npr1-5* also shows higher regeneration and the *npr3-2/npr4-2* double mutant shows no significant change from wild type in constitutive post-injury treatment. *npr1-5* shows insensitivity to constitutive post-injury treatment with either CNQX and PAMD, which are not significantly different from *npr1* Mock-treated regeneration rates. The error bars are proportional to the standard error of the pooled percentage computed using binomial distribution. (Chi-square test; $n \geq 18$; ^a significant difference with respect to Col-0 Mock, $*p < 10^{-8}$, $**p < 10^{-15}$; ^b significant difference with respect to *npr1-5* Mock, $*p < 10^{-6}$). **E.** Root regeneration frequencies of the *glr1.2/1.4/2.2/3.3* mutant in Mock and constitutive post-injury treatments, showing resistance to SA inhibitor PAMD and exogenous SA treatment. Regeneration of *glr1.2/1.4/2.2/3.3* is lower, not higher on PAMD (Chi-square, $n=40$, $p < 0.01$). SA inhibits regeneration of

glr1.2/1.4/2.2/3.3 (Chi-square, n=45, p<0.01). **F.** SA treatment significantly affects root regeneration capacity in wild type (Chi-square test; n=45; *p<0.04).



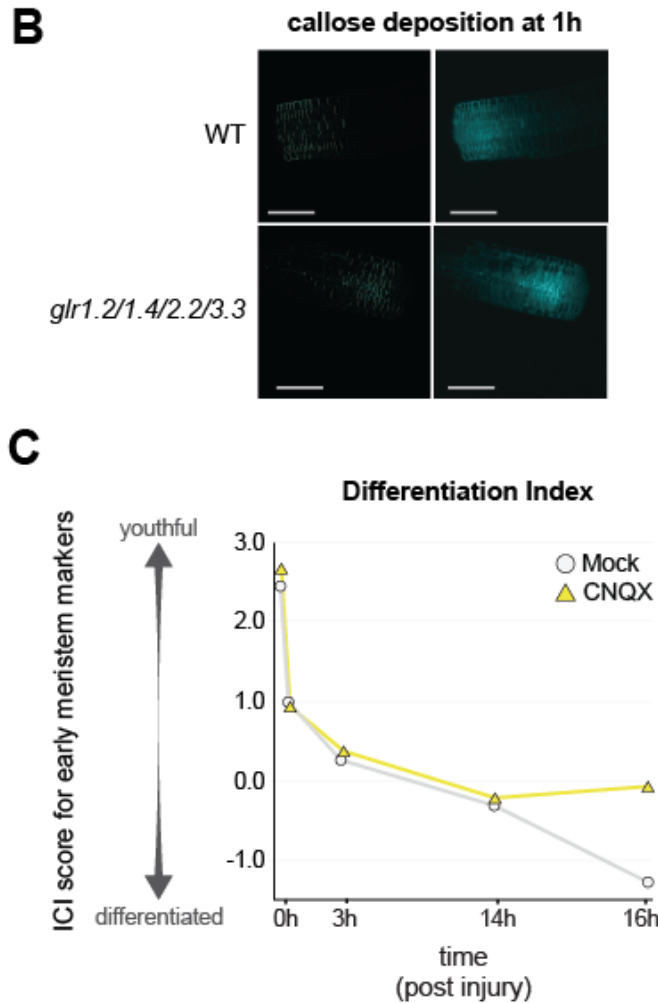


Figure S6. Related to Figure 6. Basal extracellular Ca²⁺ flux measurements, callose deposition over long term, and cellular reprogramming **A.** Extracellular Ca⁺ fluxes were measured along the root's meristematic zone for 15 min and were averaged both in wild type and *glr1.2/1.4/2.2/3.3* mutant. There is no statistically significance of basal Ca²⁺ fluxes between the two genotypes, although there is a trend of higher influx in the mutant (Welch's t test $p=0.1705$). The result shows that much stronger effects are apparent in the mutant after injury. **B.** Callose deposition in the root tip at 60 minutes post-cut, showing similar levels of callose deposition between the *glr1.2/1.4/2.2/3.3* mutant and Col-0 wild type. **C.** Cell identity analysis using a ratiometric test for markers of early-stage meristematic cells (stem cell identities) vs. late-stage differentiation (log₂ ratio), such that higher values indicate stem cell niche and early meristem identity. CNQX treated roots show higher meristem/stem cell niche identities than untreated Mock roots at 16 h post injury.

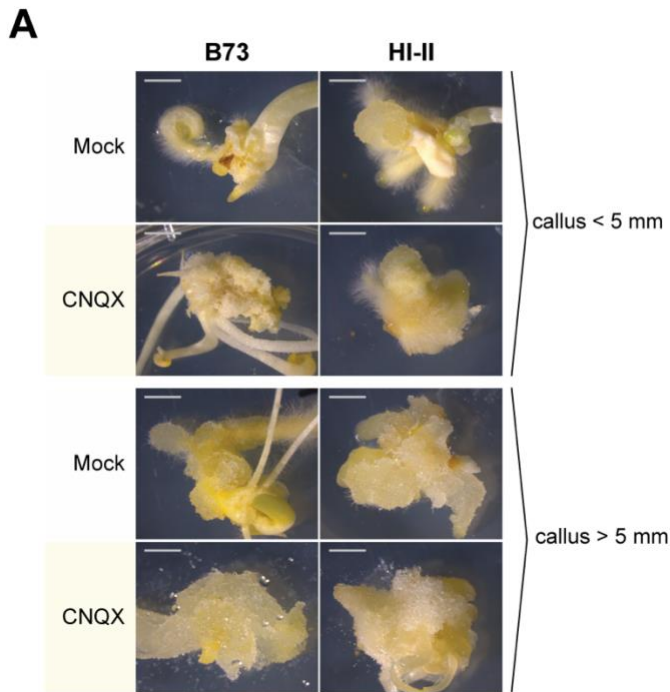


Figure S7. Related to Figure 7. Callus formation in maize HI-II and B73 lines exposed to CNQX. A. Constitutive post-injury treatment with CNQX increased the mass of cytoplasmically clear cells. Note that images from Figure 7B are re-used in this panel to provide a full comparison. Scale bar=2mm. **B.** Callus formation from single-celled protoplasts. The addition of CNQX to the media increases formation of microcalli (Chi-square test; number of cells= 8×10^4 ; where frequency of callus formation was estimated from hemacytometer readings of 3 samples from each of two biological replicates and extrapolated; $*p < 10^{-9}$). Scale bar=2mm.

